ELSEVIER

Theoretical and Applied Fracture Mechanics 31 (1999) 163–172

theoretical and applied fracture mechanics

www.elsevier.com/locate/tafmec

Three-dimensional fractal analysis of concrete fracture at the meso-level

A. Carpinteri, B. Chiaia, S. Invernizzi *

Department of Structural Engineering, Politecnico di Torino, 10129 Torino, Italy

Abstract

The fracture process in concrete-like materials cannot be properly modelled in an Euclidean framework, due to its complex morphology at the micro- and meso-level. The inherent flaws interact through a multi-scale process, leading to self-affine fracture surfaces. Moreover, the self-organized network of microcracks displays fractal properties prior to the formation of the final fracture surface. At the same time, due to the presence of pores and voids, the stress-carrying cross section is a rarefied fractal domain, even from the beginning of the loading process. A new experimental equipment has been developed which allows the entire fracture surface, or any plane cross section, to be digitised and analysed. This represents an important progress with respect to the study of one-dimensional profiles. In this paper, the three-dimensional algorithms for evaluating the fractal dimension of invasive surfaces and lacunar sections are described. The invasive fractal character of the fracture surfaces is confirmed. Moreover, the lacunar fractal character of the stress-carrying cross sections, a priori assumed by Carpinteri [A. Carpinteri, Mechanics of Materials 18 (1994) 259–266], is now proven experimentally.

1. Introduction

The disordered microstructure of concrete is responsible for many peculiar features of the fracture phenomenon. For example, size effects are not fully explicable in the classical framework. Pre-existing pores, debonded zones and microcracks interact with each other in a complex manner. Attempts to describe this behaviour by means of deterministic methods (e.g. continuum mechanics or micro-mechanics) are deemed to be incomplete if not even misleading. Even the most sophisticated measurement of material properties, coupled with the most powerful computers, would not succeed in the deterministic modelling of the fracture phenomenon. On the other hand, randomness alone cannot justify the self-organised complexity which comes into play in the fracture of concrete. On the contrary, the scale-invariant features can be put into evidence by approaching the problem from a completely new viewpoint [2].

Cooperative phenomena are now-a-days successfully interpreted by means of alternative methods, such as catastrophe theory, fractals, renormalization group and chaos theory. Modelling the microstructure by means of fractal domains permits to capture the hierarchical aspect of damage accumulation and crack propagation. It is now-a-days established that the fracture surfaces of concrete are invasive self-affine fractals over a broad scale range. This implies that the stress-singularity at the tip of a propagating crack is

* Corresponding author. Fax: +39 115 644 899; e-mail: inverns@polito.it

0167-8442/99/$ – see front matter
PII: S0167-8442(99)00011-7

smoothened and that the energy is dissipated over a higher-dimensional domain. In this context, the size effect on fracture energy and the crack-resistance behaviour can be both explained [3]. Another aspect of the same problem is represented by the lacunarity of the porous stressed microstructure, which represents a rarefied random field and can explain the size effect on the nominal tensile strength [1].

In this paper, an innovative experimental methodology is described. By means of a completely automatic laser system, the three-dimensional morphology of the fracture surfaces can be digitised. Application of three-dimensional fractal algorithms to these domains confirms the invasive character of the concrete fracture surfaces. In addition, if planar cross sections of the virgin material are considered, the pore and void distribution (like the moon-craters distribution) can be easily extracted from the laser-scanned topography. This procedure, which yields the effective depth and shape of the pores, permits to overcome the drawbacks and ambiguities of traditional image analysis techniques, where dark particles often confuse with pores. Several analyses have been carried out, confirming the lacunar fractal character of the concrete ligament, before and after loading. The same investigation allows to highlight the self-similar character of the pore size distribution, which has been assumed in various statistical models of brittle fracture [4].

2. Experimental set-up

A new experimental methodology has been developed at Politecnico di Torino, with the purpose of overcoming some major limitations commonly encountered with the existing techniques. The new set-up, infact, permits to acquire the entire surface topography, which is necessary for a real three-dimensional fractal analysis. In the literature, the fractal dimension of rough surfaces is usually calculated by simply extrapolating the values of the fractal dimension obtained from vertical sections (profiles) or from horizontal sections (as in the slit-area method [5]). The relation that links the fractal dimension of a set with that of its subsets is demonstrated only in the case of mathematical fractals, not in the case of natural fractals. In any case, if Δ is the fractal dimension of the surface and d is the (mean) fractal dimension of some profiles, one can only state that $\Delta \geqslant d+1$. Another advantage of the new technique is to avoid the ambiguities of traditional image analysis techniques, where dark particles often confuse with pores.

The experimental equipment is schematically described in Fig. 1. The specimen to be analysed is rigidly framed into a solid truss. The surface heights measurement is performed by means of a Keyence ^{TM} LB-12 laser profilometer, by counting the number of wave-cycles between the ray emission and the ray reception after the reflection on the specimen surface. The sensitivity of the profilometer has to be properly set according to the reflective optical properties of the surface to be digitized. The laser is driven by two orthogonal micrometric step-motors (UE30CC: UT 100-100), controlled by the MM2000 interface (Newport Klinger^{TM}) plugged in an ISA-slot of a PC motherboard. The analogical signal provided by the LB-72 laser controller is converted in a 16-bit precision digital signal by the DAQ PC-LPM-16 data acquisition board (National Instruments^{TM}). A dedicated software provides extreme versatility and the full automation of the surface acquisition process. The digitised surface can extend over a 50 mm $\times$ 100 mm area, and a maximum precision of 2 μm can be achieved, both in vertical and horizontal directions.

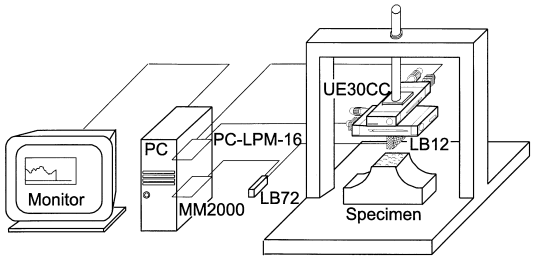

Fig. 1. Experimental equipment: monitor, PC case, data acquisition board PC-LPM-16, step-motors board MM2000, laser controller LB72, concrete specimen, laser pointer LB12, step-motors UE30CC.

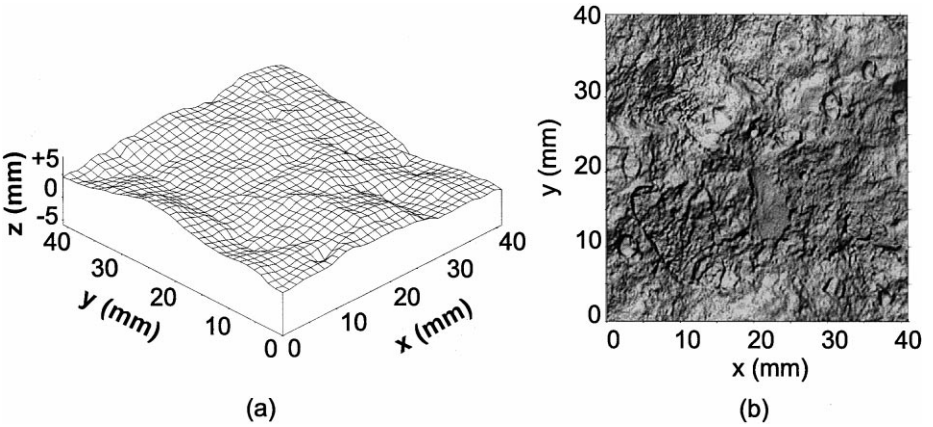

Fig. 2. Digitised fracture surface: three-dimensional wireframe view (a); shaded relief (b).

Several concrete fracture surfaces, obtained from uniaxial tension tests, have been digitised. One of them is shown in Fig. 2. This surface extends over a $4 \times 4\,\mathrm{cm}^2$ projection area, and has been stored as a 2048×2048 pixel array. Therefore, a 20 μm digitization step was adopted. It is believed that further refinements are not necessary for the meso-structural characterisation of concrete-like materials. The surface is extremely rough and shows more and more details as the observation resolution increases. Moreover, the same morphology is observed under different magnifications. This confirms a substantial scale-invariance. As will be shown in the following, the scale-dependent value of the apparent area tends to infinity as the resolution increases. Therefore, it is not consistent to deal with this domain as it were a smooth Euclidean surface.

Furthermore, planar concrete cross sections have been digitised. They were obtained by cross-cutting undamaged specimens. In the case of Fig. 3(b), a 1024×1024 pixel array was stored,

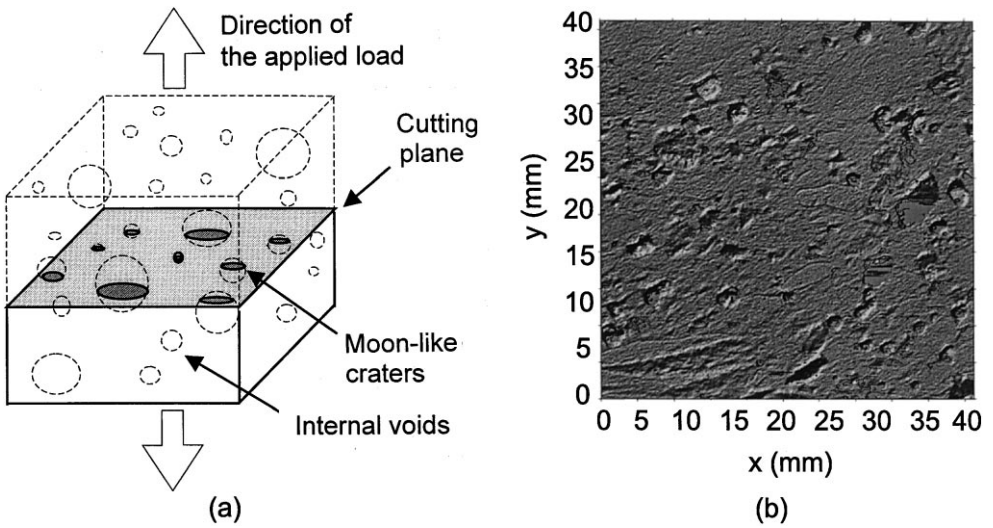

Fig. 3. Voids structure scheme (a); shaded relief of a digitised stress-carrying section obtained by cross-cutting the undamaged concrete specimen (b).

and a 40 μm resolution was adopted. These surfaces appear almost flat, with localised distribution of moon-like craters due to the intersection of the cutting plane with the pre-existing microstructural voids (Fig. 3(a)). Therefore, the effective resistant cross section is less dense and compact than the nominal cross section. In the case of uniform porosity, referring to the nominal cross section does not provide scaling effects. However, in the real situations, as will be outlined in the following, the porosity is not uniform, and the relative percentage of voids depends on the cross section linear size. Thus, scale effects come into play.

3. Invasive fractality of the fracture surfaces

The digitised fracture surfaces have been analysed by using three different algorithms (and the corresponding mathematical definitions) for the fractal dimension evaluation. Based on the classical concept of covering dimension, originally used by Mandelbrot [5], the box-counting method allows to calculate the fractal dimension of lacunar and invasive fractal sets. The fracture surface is assumed to be an invasive self-affine fractal in a statistical sense. This means that a three-dimensional representation of the surfaces $f(x,y,z)$ will be statistically similar to $f(rx,ry,r^{H}z)$, where r is the scaling factor and H is the Hurst exponent due to the anisotropy in the scaling procedure.

As shown in Fig. 4(a), the fractal dimension can be evaluated from the rate of growth of the number N of prisms, necessary to cover the entire surface, as the size d of the elementary prisms (whose volume is $V = d \times d \times d^{H}$) decreases. The following equation holds:

$$\Delta_{box} = \lim_{d \to 0} \frac{\log N}{\log(1/d)}. \quad (1)$$

From a practical point of view, the fractal dimension can be evaluated from the slope of the regression straight line in the bi-logarithmic diagram $\log N$ vs. $\log d$ (Fig. 4(b)). The fractal dimension of the surface shown in Fig. 2, calculated according to Eq. (1), is equal to $\Delta_{box} = 2.15$, and confirms the invasive fractal nature of this domain.

While the box-counting algorithm estimates the fractal dimension from the rate of vanishing of the overall covering volume as the resolution increases, the patchwork method approximates the fractal domain (which is inherently non-differentiable) by surface elements (Fig. 5(a)). The fractal dimension is evaluated from the rate of divergence of the apparent area A as the size of the surface elements decreases. In other words, the patchwork method aims at evaluating the same limit value, i.e.the fractal dimension, by approximating it from a different path. For example, when the covering grid size is $r = 20.48$ mm, then the apparent area A is equal to 1698.17 mm^2 (whereas the nominal area is equal to $40 \times 40 = 1600$ mm^2). By increasing the

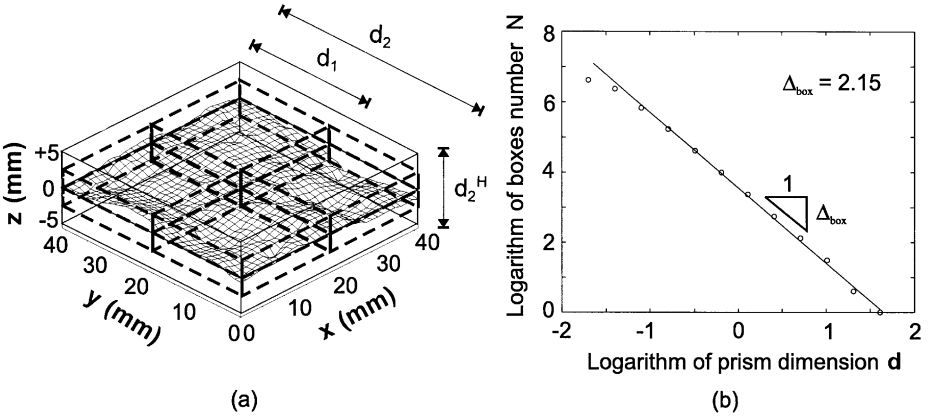

Fig. 4. Box-covering scheme (a); bilogarithmic diagram (b).

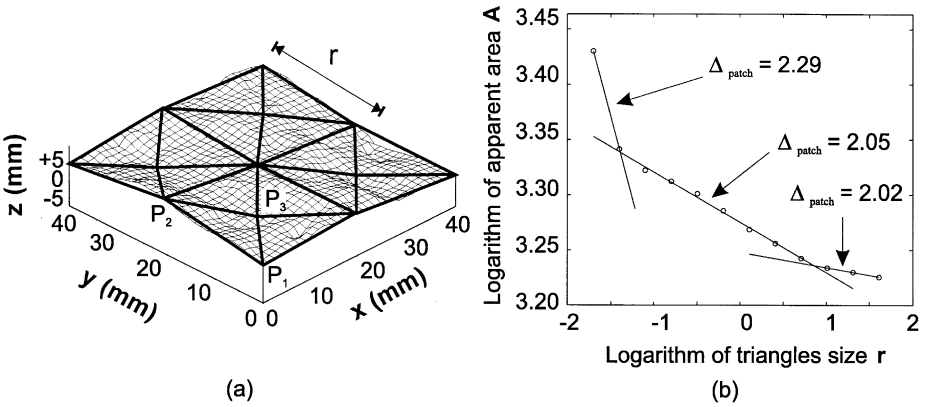

Fig. 5. Triangulation approximation scheme (a); bilogarithmic diagram (b).

resolution, more and more details are counted and, when $r = 20$ μm, A becomes equal to 2691.39 mm^2. This confirms the scale dependent nature of the Euclidean description. The patchwork fractal dimension, originally defined by Clarke [6], can be computed as:

$$\Delta_{\text{patch}} = 2 - \lim_{r \to 0} \frac{\log A(r)}{\log r}. \tag{2}$$

In Fig. 5(b), the bilogarithmic diagram $\log A$ vs. $\log r$ is shown for the surface in Fig. 2. The fractal dimension, equal to the slope of the curve, is correctly evaluated only for high resolution (local fractal dimension). On the contrary, it tends to the Euclidean integer value for poor resolution, due to the self-affine character of the considered surfaces.

Finally, the fractal dimension of the fracture surfaces has been calculated by a three-dimensional spectral method, specifically designed for self-affine sets [7]. It is based on the two-dimensional Fourier Transform H_{st} of the fracture relief, which is shown in the logarithmic diagram of Fig. 6(a). The method provides the fractal dimension as a function of the mean spectral power S_{2j}, which can be calculated as:

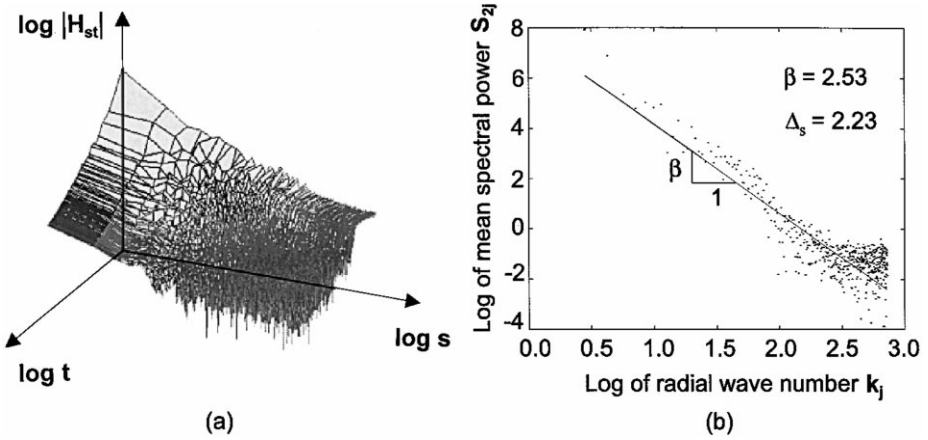

Fig. 6. Tri-logarithmic diagram of the absolute value of the bi-dimensional Fourier transform (a); bilogarithmic diagram of the mean radial power spectrum (b).

$$S_{2j} = \frac{1}{l^2 N_j} \sum_{1}^{N_j} |H_{st}|^2, \tag{3}$$

where l is the linear size of square digitized area and N_j is the number of points that satisfy the condition $j < (s^2 + t^2)^{1/2} < j + 1$. For self-affine surfaces, the mean spectral power obeys the following power-law:

$$S_{2j} = k_j^{-\beta-1}, \tag{4}$$

where k_j is the radial wave number and β is the slope of the curve in the $\log S_{2j}$ vs. $\log k_j$ bilogarithmic diagram shown in Fig. 6(b). The spectral fractal dimension can be obtained as a function of β:

$$\Delta_S = \frac{7 - \beta}{2}. \tag{5}$$

The spectral method provides the value $\Delta_S = 2.23$ for the same surface shown in Fig. 2.

In conclusion, the dimension of this surface should be set in the range 2.15–2.29. Unfortunately, in the case of natural fractals, it is difficult to obtain a well-defined value because the algorithms, although in principle coincident in the theoretical limit, behave differently when applied to real sets.

4. Lacunar fractality of the stress-carrying cross sections

In the study of continuous media, we are concerned with the manner in which forces are transmitted through the medium. The Cauchy definition of stress relies on some "regularity" properties (continuity and measurability) of the medium. However, heterogeneities and defects are present at all the scales in engineering materials and interact with each other in a complex manner. These aspects cannot be neglected when meso- or micro-scales are considered, and in the presence of strain localization and large stress gradients, which is the case for fracture and contact problems. Carpinteri [1] assumed that the fractal dimension of stressed ligaments in disordered solids were lower than 2.0 due to voids and cracks. Therefore, in his approach [1,2], lacunar domains (possessing a fractal dimension lower than the topologic dimension) were used to model the stress-carrying cross sections of real materials. The apparent Euclidean measure (length, area or volume) of lacunar sets is scale-dependent and tends to zero as the resolution increases. Therefore, the Cauchy definition of stress could not be applied. The "regularity" properties of the Euclidean sets should be lost and replaced by the non-differentiability. On the other hand, self-similarity comes into play, providing a particular symmetry in the problem (dilatation symmetry). Accordingly, the stress concept has to be drastically revised and scaling laws should be included in the definition of material strength [1,2].

The Menger sponge can be considered as the archetype of a lacunar fractal solid. It is shown at the third iteration in Fig. 7(a), and its Hausdorff dimension is equal to $\Delta = \log 20/\log 3 = 2.73$. The sponge has zero volume and possesses very peculiar mass properties related to its non-compactness. In fact, if sponges of different linear size are compared, one notes that the nominal density decreases with size according to a non-integer exponent equal to $D - 3$. This is confirmed by natural sponges, where the larger the specimen size, the higher the probability of encountering a large hole. Planar cross sections of the Menger sponge are Sierpinski carpets, whose iteration scheme is shown in Fig. 7(b). This set presents zero area ($\Delta = \log 8/\log 3 = 1.893$) and can be considered as a lacunar cross section inside a porous medium.

In the presence of brittle fracture, the energy dissipation domain can be directly identified with the digitized fracture surface. Instead, the

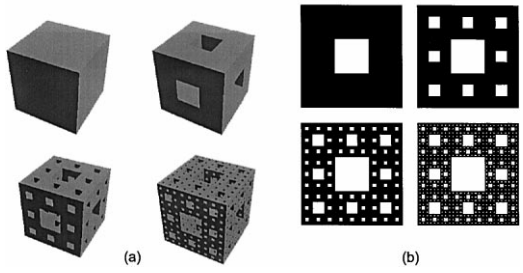

Fig. 7. Iteration scheme of the Menger Sponge (a) and of the Sierpinski Carpet (b).

determination of the effective cross section requires some further analyses. The true stressed domain is made out of the points that do not belong to the craters, i.e.to the pore structure. Hence, from a theoretical point of view, the actual resisting cross section can be evaluated by considering the set of points whose heights are exactly equal to the cutting plane height. Practically, the obtained surface (Fig. 3(b)) is not absolutely planar and presents a low uniform roughness, due to the cutting process, that can be confused with the pre-existing porosity. For this reason, another virtual plane has been considered, parallel to the cutting section but at a slightly lower level, which is able to intersect only the real cavities (Fig. 8(a)). Thereby, only the points whose heights are larger than the virtual plane height are considered to belong to the real stress-carrying domain. The remaining points belong to the (complementary) void set. This procedure allows to filter out the noise produced by cutting. However, some information is lost about the finer porosity. To perform the virtual cut, it is also necessary to determine the mean cutting plane by a de-trending algorithm. Fig. 8(b) shows the processed cross section, starting from Fig. 3(b), where the black pixels represent the real stress-carrying domain before the application of the load.

The fractal dimension of this domain has been calculated by using two different algorithms. The first is the previously introduced box-counting method. The number of boxes needed to cover the set has been calculated for increasing resolutions. Because the considered set is approximately isotropic (self-similar scaling), square covering elements of decreasing size d can be used (Fig. 9). The effective ligament presents a fractal dimension equal to $\Delta_{box} = 1.92$ (Fig. 11(a)), clearly lower than the integer value ($D = 2.00$), which is valid for compact Euclidean sets.

The fractal dimension of the stress-carrying domain can be also evaluated by referring to the mass logarithmic density. When dealing with perfectly homogeneous sections (Fig. 10(a)), the density can be conventionally assumed equal to one. Moreover, if the effective cross sections were characterized by a uniform distribution of cavities (Fig. 10(b)), it would be possible to calculate the density defined as the ratio, lower than one, of the effective area A_{eff} to the nominal area A_{nom}. In the case of uniform porosity, a characteristic length scale can be easily determined and therefore, given an appropriate resolution, a size-independent value of the density is obtained. Instead, in the case of the true domain (Fig. 10(c)), this density cannot be unambiguously calculated because it inherently depends on the adopted resolution and on the size of the considered area. In fact, the self-similar distribution of the pores at all the scales causes the probability of finding large cavities to be higher as the size of the considered area increases (as for natural sponges [5]). The classical density is therefore not constant, but decreases by increasing the nominal size of the domain. To obtain a scale-invariant value, it is necessary to refer to the logarithmic density, defined as:

$$\rho_{log} = \frac{\log A_{eff}}{\log A_{nom}}. \tag{6}$$

If d is the linear size of the considered area, the fractal dimension Δ_{log} can be evaluated as the limit

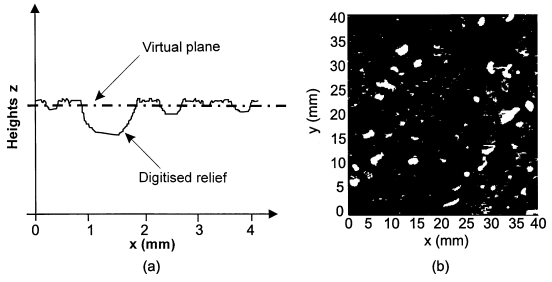

Fig. 8. One-dimensional scheme of the virtual plane position (a); effective stress-carrying cross section (b).

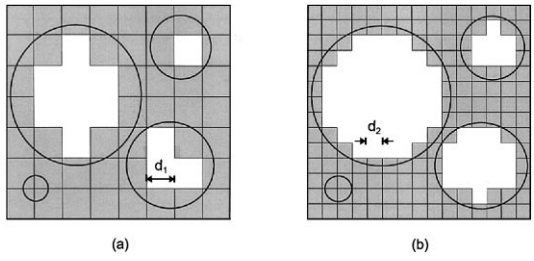

Fig. 9. Covering scheme for the *Box Counting Method* applied to a lacunar set embedded in the plane.

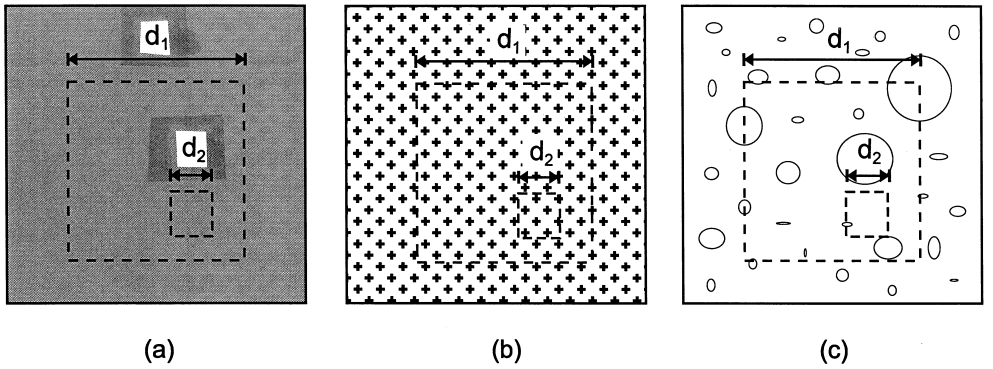

Fig. 10. Homogeneous micro-structure (a); uniform porosity (b); complex voids structure (c).

slope of the bilogarithmic diagram ($\log A_{\text{eff}}$ vs. $\log d$). In the case of concrete (Fig. 11(b)), the value $\Delta_{\log} = 1.92$ was determined, in good agreement with the box-counting method.

In Fig. 12, the variation of the fractal dimension of the effective cross section is shown as a function of the virtual plane height. It is worth noting the rather sharp decrease of the dimension as the cutting noise comes into play, even if there is a certain amount of uncertainty in the choice of the virtual plane position. If one were able to quantify the effect of this noise, the virtual plane height would be unequivocally defined.

As a final remark, it is our opinion that the value $\Delta = 1.92$ is too high, even for an undamaged specimen. Higher resolutions in the digitization procedure should reveal the presence of micro-porosity, which would drastically lower the density and the compactness of the stress-carrying domains.

Another interesting issue to be investigated is represented by the evolution of the stress-carrying domain during the loading process. Before the application of the load, the domain ($\Delta = 1.92$) is affected only by the pre-existing material porosity. Afterwards, as the load increases, nucleation of new flaws as well as their coalescence lowers furtherly the compactness of the set. It is easy to realize that, as the domain becomes more and more rarefied, both its fractal dimension and its fractal measure (L^{Δ}) will decrease. When the final separation occurs, both these values should vanish. It might be argued that, if the topology evolution of the stress-carrying domain were detectable step by

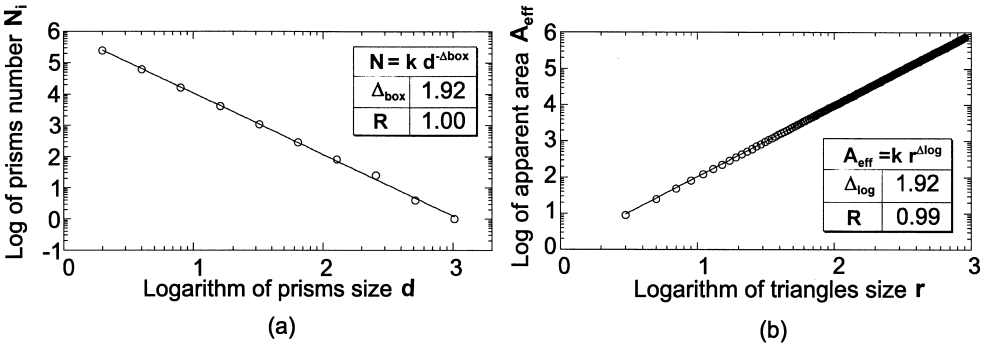

Fig. 11. Bilogarithmic diagrams for the number of covering boxes (a) and of the apparent mean area (b) as functions of the resolution step.

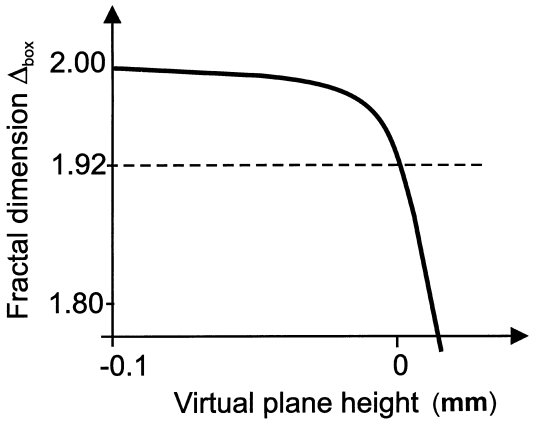

Fig. 12. Fractal dimension of the stress-carrying cross section as a function of the virtual plane height.

step, a scale-independent constitutive law, valid in the elastic and softening regimes, could be determined for concrete-like materials [8].

5. Conclusions

The classical theories in strength of materials are used to define two characteristic quantities, respectively the nominal tensile strength and the apparent fracture energy. Both values are assumed to be invariant with respect to the structural size. Moreover they are both obtained by normalizing the maximum tensile load, or the overall amount of dissipated energy, with respect to an ideal (compact and smooth) cross section area, as depicted in Fig. 13(a).

As now-a-days widely recognised, these hypotheses are acceptable only in a first approximation. In fact our experiments show that the effective energy dissipation domain is not an Euclidean flat surface (Fig. 13(b)) and that, on the other side, the stress-carrying cross section is more rarefied than the nominal area (Fig. 13(c)). Consequently, the classical definition of the material properties are not scale invariant. While, from an experimental point of view, the phenomenon of scale effects has been unequivocally recognised, there are different theories, sometimes in disagreement with each other, which intend to explain this anomalous behaviour.

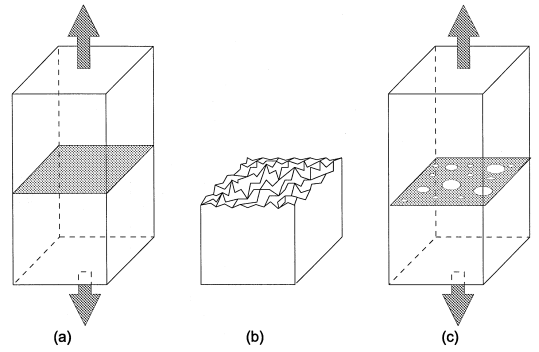

Fig. 13. Classical homogeneous stress-carrying cross section and euclidean energy dissipation domain (a); effective energy dissipation domain (b); true stress-carrying cross section (c).

Carpinteri [1] proposed to approach the problem from a completely new point of view, by considering the effective nature of the energy dissipation domain and of the stress-carrying cross section. In this case, in agreement with the Renormalization Group Theory, the new mechanical properties present anomalous physical dimensions and are invariant with respect to the structural size. The fractal hypothesis for the microstructure of the material has been fully confirmed by the experimental results of the present work.

It is worth noting that, when broader dimensional ranges are taken into consideration, the mono-fractal modelling is only a local approximation. In this case, it is necessary to consider a continuous transition from the local fractal dimension, that holds at the small scale, to the global dimension that is equal to Euclidean topological dimension. The transition from the disordered regime, at small scales, to the ordered regime, at large scales, is correctly described by the Multifractal Scaling Laws [9] for the apparent fracture energy (Fig. 14(a)) and for the nominal tensile strength (Fig. 14(b)). These scaling laws cover the entire scale range and can be used for extrapolating experimental properties from small-sized specimens to full-scale structures.

Acknowledgements

The present research was carried out with the financial support of the Ministry of University and

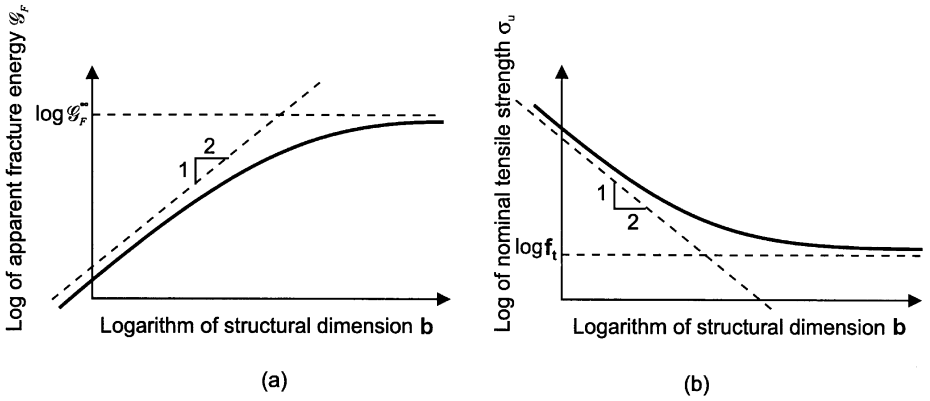

Fig. 14. Scaling behaviour of the nominal fracture energy (a) and of the nominal tensile strength (b).

Scientific Research (MURST), the National Research Council (CNR) and the EC-TMR Contract N^o ERBFMRXCT 960062.

References

[1] A. Carpinteri, Fractal nature of material microstructure and size effects on apparent mechanical properties, Mechanics of Materials 18 (1994) 259–266; also Internal Report, Laboratory of Fracture Mechanics, Politecnico di Torino (1992).

[2] A. Carpinteri, B. Chiaia, Power scaling laws and dimensional transitions in solid mechanics , Chaos, Solitons and Fractals 7 (1996) 1343–1364.

[3] A. Carpinteri, G. Chiaia, Crack-resistance behavior as a consequence of self-similar fracture topologies, International Journal of Fracture 76 (1996) 327–340.

[4] A. Carpinteri, B. Ferro, S. Invernizzi, The nominal tensile strength of disordered materials: a statistical fracture mecanichs approach, Engineering Fracture Mechanics 58 (1997) 421–436.

[5] B.B. Mandelbrot, The Fractal Geometry of Nature, Freeman, San Francisco, 1982.

[6] K.C. Clarke, Computation of the fractal dimension of topographic surfaces using the triangular prism surface area method, Computer and Geosciences 12 (1986) 713–722.

[7] D.L. Turcotte, Fractal and Chaos in Geology and Geophysics, Cambridge University Press, Cambridge, 1992.

[8] A. Carpinteri, G. Ferro, Scaling behaviour and dual renormalization of the experimental softening responses, Materials and Structures 31 (1998) 303–309.

[9] A. Carpinteri, B. Chiaia, Multifractal scaling laws in the breaking behaviour of disordered materials, Chaos, Solitons and Fractals 8 (1997) 135–150.